

# RAY TRACER FOR ANALYSIS OF SOLAR CONCENTRATING SYSTEMS

Karidewa Nyeinga<sup>1</sup>, Eldad J.K.B. Banda<sup>1</sup>, Ole J. Nydal<sup>2</sup>

<sup>1</sup>Department of Physics, Makerere University, P.O. Box 7062, Kampala, Uganda.

<sup>2</sup>Department of Energy and Process Engineering, NTNU, P.O. Box 7491, Trondheim, Norway.

## Abstract

Solar concentrating systems are designed to provide solar energy at high temperatures. The sizes of solar systems range from large scale power plants to small scale household systems, where thermal heat is collected for heating and cooking purposes. A ray tracer can be useful when designing the reflection and absorption components of solar concentrators, in particular for complex systems with several components in a non symmetric 3D arrangement. Emitted sun rays are traced from the source through all reflections until they intercept with the receiver or are lost past all of the components. A 3D ray tracer method to simulate and analyze solar concentrating systems is presented. The algorithm of the ray tracer and a vectorized implementation of it (in MATLAB) is presented. The ray tracer has been programmed as part of an effort to develop small scale concentrating solar energy systems with integrated heat storage units. The ray tracer is demonstrated for selected cases where a comparison between continuous reflecting surfaces and flat mirror tiled surfaces is made. Off focus sensitivity analysis can provide guidelines for the required solar tracking accuracy. Sensitivity analysis on the size of mirror tiles can be made, in relation to the absorber geometry. Ray tracing computations have in particular been useful when analyzing double reflection systems, where a primary reflector with focus on a secondary reflector which focus further onto the absorber. Such systems become sensitive to the accuracy and to the geometry of the reflecting elements.

## 1. Introduction

Solar thermal energy storage systems designed to operate at high temperatures require concentrating collectors. A solar concentrator consists of one or more reflectors mounted to face the sun and reflect or ‘concentrate’ the solar radiation on to a receiver placed at the focal point of the reflector (Duffie and Beckman, 2006). The main challenge from a practical point of view encountered in solar concentrating systems is that the temperature distribution on the absorbers is not uniform and this affects the inlet fluid temperature; and hence the charging of the bed. Effective charging demands that inlet fluid temperatures to be maintained or increased (Chikukwa, 2007).

Ray tracing is a technique of following the path of an incident ray from the source to the final point. The advantage of using ray tracing is its ability to handle any kind of geometry and still provide complete visibility (Seron et. al, 2005). An accurate beam distribution analysis gives an insight into the design of reflectors and receivers. Ray tracing tool is finding growing use in different research areas. Spencer and Murty (1962) describe a unified procedure of ray tracing applicable to optical systems containing cylindrical and surfaces of arbitrary orientation and position. Zeng et al. (2003) used ray tracing method to simulate a sound field. Yevgen and Yuriy (2007) used Monte-Carlo ray tracing to simulate light scattering in spherical clusters of large transparent particles. Stephen et al. (2010) presented work based on ray tracing to study how well non-imaging daylight collector pipes diffuse light into long horizontal funnels for illuminating deep buildings. Te-Tan (2009) presented a study based on ray tracing techniques to examine the errors induced in a light ray’s path as it is reflected or refracted at a paraboloidal boundary surface and concluded that using ray tracing method, the effect of the light path in each boundary surface within the optical system can be systematically examined. Duffie and Beckman (2006) give a brief outline on the application of ray tracing in solar concentrating systems. Chi-Feng et. al (2010) investigated a solar concentrator combining primary paraboloidal and secondary hyperboloidal or ellipsoidal mirrors by using a ray-tracing method to obtain higher concentration ratios. Ralf and Hans (2007) presented a method using reverse ray tracing for stationary solar concentrators with the intension of estimating the performance of photovoltaic concentrators. They explained that using ray tracing, new concentrators may be optimized for location and tilt.

This work is based on simulation of solar radiation concentrating system using ray tracing tool; it is done in 3D using MATLAB. The path of a ray is traced from the sun to the final destination; which could be a collector, receiver or even the surrounding. The collector is a parabolic dish whose surface is made of continuous surfaces or flat mirror tiles. The performance of the continuous surface reflectors is compared with that of flat mirror tiles. The effect of secondary reflectors in improving the interception factor is also discussed.

## 2. Description of the Model

We model a sun emitting rays which are reflected by parabolic dish onto a receiver placed at the focal point of the reflector. See figure 1.

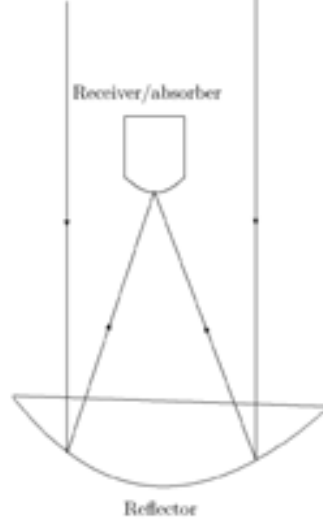


Figure 1: Schematic diagram of the concentrating system; sun rays are reflected by the parabolic dish on a receiver at the focus

- The sun: is made of panels and emits rays.
- The reflector: is a parabolic dish; the surface is either made of flat mirror tiles or continuous mirror surface.
- The receiver: different geometries are used namely flat, cylindrical, box and spherical.

## 3. Equations for the surface and Algorithm

We describe the equations and the algorithm to find the intersection of a ray on plane for a parabolic dish made of a flat panel or a continuous surface. A detailed description of the implementation of the algorithm is also presented.

### 3.1 Algorithm for a surface of flat tiles

The equation of a plane (points  $\vec{P}$  are on the plane with normal  $\vec{N}$  and point  $\vec{P}_3$  on the plane) can be written as:

$$\vec{N} \cdot (\vec{P} - \vec{P}_3) = 0 \quad (1)$$

The equation of the line (points  $\vec{P}$  on the line passing through points  $\vec{P}_1$  and  $\vec{P}_2$ ) can be written as:

$$\vec{P} = \vec{P}_1 + u(\vec{P}_2 - \vec{P}_1) \quad (2)$$

$u$  is the length of the line between the points.

The intersection of these two occurs when

$$\vec{N} \cdot (\vec{P}_1 + u(\vec{P}_2 - \vec{P}_1)) = \vec{N} \cdot \vec{P}_3 \quad (3)$$

Solving for  $u$  gives:

$$u = \frac{\vec{N} \cdot (\vec{P}_3 - \vec{P}_1)}{\vec{N} \cdot (\vec{P}_2 - \vec{P}_1)} \quad (4)$$

So we find the normal vector to the plane.

### 3.2 Algorithm for continuous surface

We consider a parabolic disc made of a continuous mirror surface and find the point of intersection of a ray with the surface. Given a focal point  $f$  on the z-axis; then it can be described by the equation:

$$x^2 + y^2 = 4fz \quad (5)$$

To find the point of intersection  $P(x, y, z)$  on the surface of a line having direction  $\vec{d}$  and starting from the point  $S(s_x, s_y, s_z)$  which is the sun. The length along the ray to the point of intersection is  $u$ .

$P$  is defined by:

$$\vec{P} = \vec{S} + u\vec{d} \quad (6)$$

On component form this is

$$x = s_x + ud_x$$

$$y = s_y + ud_y$$

$$z = s_z + ud_z$$

The shape of the surface is:

$$p = p(x, y, z) = 0$$

$$p = x^2 + y^2 - 4fz = 0$$

Inserting the components into the surface shape gives an equation for  $u$ :

$$(s_x + ud_x)^2 + (s_y + ud_y)^2 - 4f(s_z + ud_z) = 0$$

Rearranging:

$$(s_x + ud_x)^2 + (s_y + ud_y)^2 - 4f(s_z + ud_z) = 0$$

$$u^2 d_x^2 + u^2 d_y^2 + 2ud_x s_x + 2ud_y s_y - 4fd_z + u + s_x^2 + s_y^2 - 4fs_z = 0$$

$$u^2 (d_x^2 + d_y^2) + u(2d_x s_x + d_y s_y - 4fd_z) + (s_x^2 + s_y^2 - 4fs_z) = 0 \quad (7)$$

Equation (7) is a second order equation of the form:

$$au^2 + bu + c = 0$$

Where

$$a = d_x^2 + d_y^2$$

$$b = 2d_x s_x + d_y s_y - 4fd_z$$

$$c = s_x^2 + s_y^2 - 4fs_z$$

The solution is:

$$\left\{ \begin{array}{l} \left\{ -\frac{c}{b} \right\} \quad \text{if } b \neq 0 \wedge a = 0 \\ \left\{ -\frac{1}{2a} \left( b - \sqrt{-4ac + b^2} \right), -\frac{1}{2a} \left( b + \sqrt{-4ac + b^2} \right) \right\} \quad \text{if } a \neq 0 \wedge 4ac \leq b^2 \end{array} \right. \quad (8)$$

This is solved in 3D using MATLAB. There may be real solutions and no solutions or complex numbers. We solve for  $u$  and extract only the positive numbers. The rest are lost rays. The computation does not fail as long as we remove the non physical results after the  $u$  computations.

We then need the normal vector  $\vec{n}$  at point of intersection to compute the reflected rays  $\vec{r}$ .

$$\vec{r} = \vec{d} + 2\vec{n} \quad (9)$$

The normal vector is the normalized gradient of the surface:

$$\vec{n} = \frac{\nabla p}{|\nabla p|} \quad (10)$$

For a parabola, the components at the point  $P(x, y, z)$  are:

$$\nabla(x^2 + y^2 - 4fz) = 2x\vec{i} + 2y\vec{j} - 4f\vec{k}$$

$$|\nabla p| = \sqrt{4x^2 + 4y^2 + (4f)^2}$$

The procedure is then, for each surface:

- Given a sun point  $S$  and a direction of the ray  $\vec{d}$  we solve the second order equation (8) for  $u$ .
- We remove the non physical values of  $u$ , and retain only the positive values.
- The intersection point is computed from (6).
- At this point  $P$ , compute the normal vector,  $\vec{n}$ , and the reflected vector in equation (9).
- The point  $P$  becomes the new sun point and  $\vec{r}$ , the new sun direction.

After all the surfaces have been looped over, we retain only the first reflection point of the ray, in case of multiple reflections.

### 3.3 Implementation of the model

The reflectors and the receiver are discretized into small panels. The sun is discretized into several panels and each panel emits rays. For each panel, we take note of the center position which is the point where the rays are emitted from. The direction of the ray is dependent on the given sun angle. We loop over all panels and find the intersections for all rays and the selected panel/ surface. We test to ensure that the point of intersection is within the panel.

Multiple reflections are removed and the rays are sorted to remove duplicate rays. We 'kill' rays on absorbers, so that no further reflections occur from absorbers.

## 4. Results and Discussions

The tracer tool has been used to simulate different cases; reflectors made continuous and flat mirror tiles of varying aperture and focal length, receivers of different geometries, etc. Results are shown and discussed below.

### 4.1 Testing model with parallel rays

We illustrate the validity of the model with parallel rays emitted from the sun at incident normal to the aperture of the reflector. The rays are traced from the sun onto the reflector as shown in figure 2. In figure 3, all parallel rays incident on the parabolic dish are reflected to the focal point where there is a receiver. This demonstrates a case that agrees with basic theory.

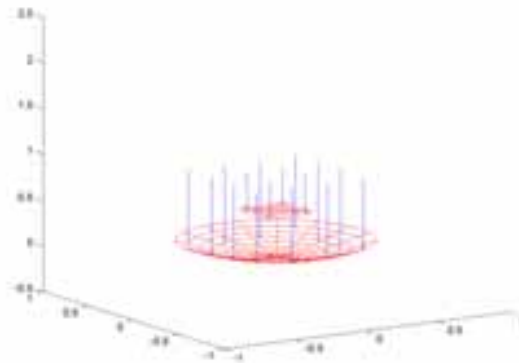


Figure 2: A beam of parallel rays emitted from the sun normal to the aperture of the reflector.

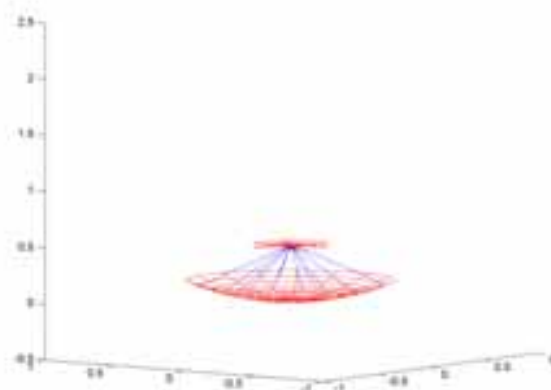


Figure 3: Parallel rays are reflected onto a receiver placed at the focal point of the parabolic dish made of continuous mirror surface.

#### 4.2 Interception Ratio

Figure 4 shows the interception ratio i.e. the fraction of the radiation incident on the aperture of the concentrator at angle  $\theta$  reaching the receiver for two types of reflectors: one made of flat mirror tiles and the other made of continuous mirror surface. For radiation incident within the acceptance angle, the fraction is unity. However, at angles above the acceptance angle, less radiation reaches. It is observed that a concentrator made of continuous reflecting surface has a wide range of acceptance angle compared to that made of flat tiles. However, the fraction falls sharply for the continuous surface for radiation incident outside the acceptance angle.

The high acceptance angle for the reflector with continuous surface implies that it is possible for such concentrator to function with minimum requirements for tracking since it has the ability to reflect to the receiver all of the incident radiation within the limits of the acceptance angle. To improve the performance of the interception ratio for the flat tiles, the size of each tiles has to be reduced which is a challenge in practice.

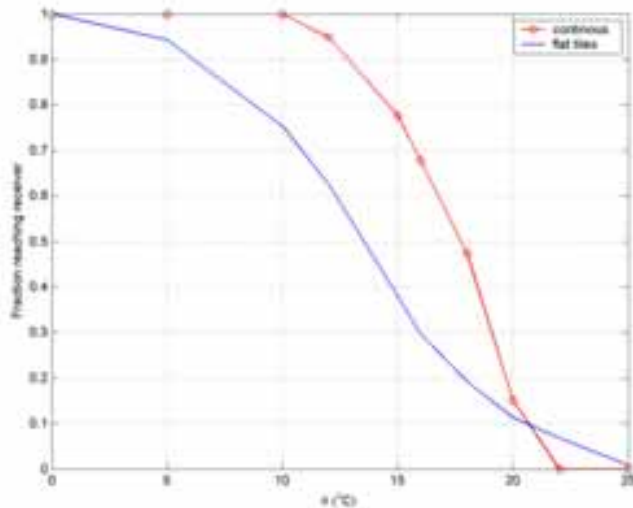


Figure 4: Fraction of incident radiation on the aperture of the parabolic dish reaching the receiver for concentrator made of continuous surface and flat tiles.

#### 4.2 Images on the receiver for varying angles of incident radiation

Angle variations in the incident radiation on the aperture of a continuous reflecting surface and the image of the reflected beam on the receiver are shown in figures 5-7; the number of hits per absorber area is used. In figure 5, the incident radiation is at angle  $0^\circ$  depicting a very good tracking system. Therefore, all the radiation is concentrated at the focal point on the receiver and hence the observed image at the center of the receiver showing very high hits per absorber area. The rest of the receiver parts do not receive any radiation.

Figures 6 and 7 demonstrate cases where the incident radiation is not normal to the parabola aperture and the reflected beam is observed to shift from the focal point (at the center) towards the edge of the receiver. The intensity of the radiation (which is illustrated by the number of hits per unit area) reduces as well and it is not concentrated at one point; at  $15^\circ$  most of the radiation is lost. This illustrates a case of poor tracking. Errors in tracking lead to fall in intensity of the radiation/energy concentrated on the receiver.

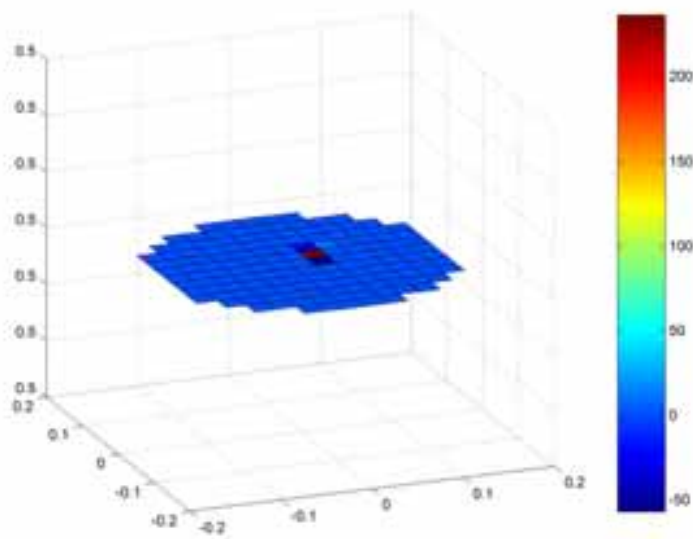


Figure 5: Radiation incident at zero degree; showing an example of very good tracking system. All the rays are concentrated at the center and therefore high absorber hits per area (intensity) is observed.

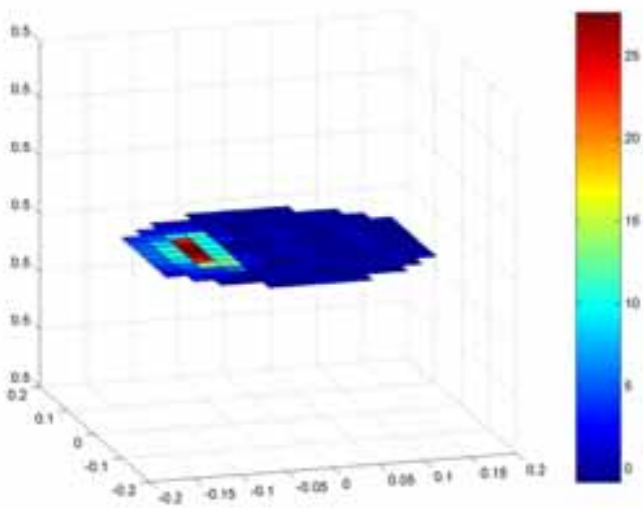


Figure 6: Radiation incident at 10 degree; a case of poor tracking. The reflected rays fall at points away from the focal point and the intensity is low

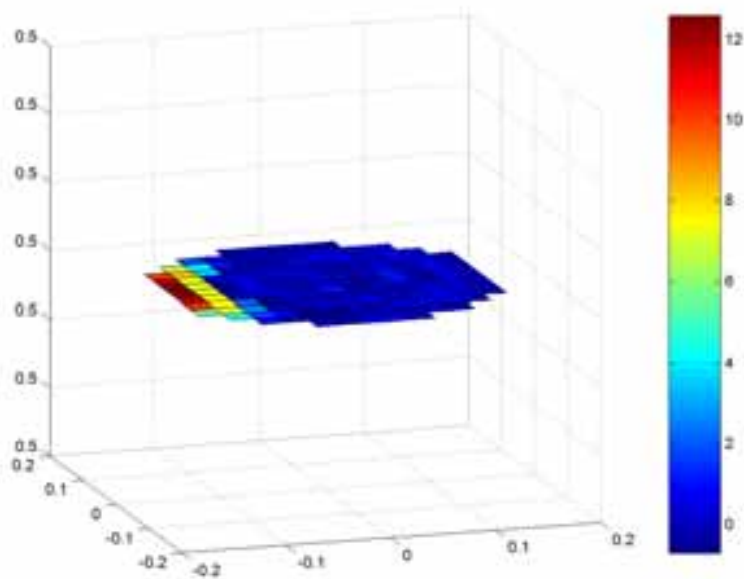


Figure 7: Radiation incident at 15 degree showing very poor tracking. The reflected rays only hit the edges of the receiver. No concentration and the intensity (the number of hits per absorber area) are very low.

#### 4.2 Secondary Reflector

A secondary reflector with focal point on the receiver is introduced to intercept rays from the primary reflector that do not hit the receiver and reflects them back onto the receiver. Figure 8 shows the use of secondary reflector to enhance the concentration of the beam on the receiver. The impact of having a secondary reflector becomes important when the system is out of focus as shown by the increased interception ratio.

In practice it is difficult to maintain the concentrating system in focus due to challenges in the tracking mechanism. For a system designed for rural communities, mechanical tracking is usually recommended, however, such a system does not track very well and therefore a secondary reflector could be used to improve the overall concentration. But it should also be noted that the increased interception ratio observed due to the secondary reflector may not translate into increased energy in the absorber due to losses in energy as a result of multiple reflections between the primary and the secondary reflector. Therefore, an experiment is needed to find the impact of the secondary reflector in terms of the energy at the receiver.

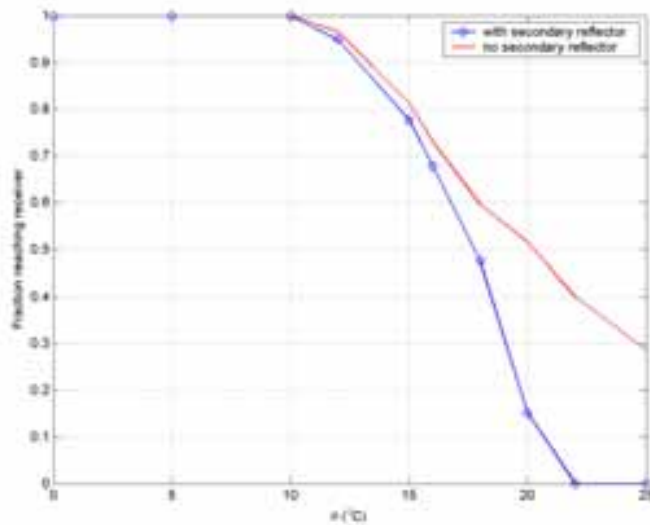


Figure 8: A secondary reflector improves the interception ratio although experimental measurements are needed to check whether there is an increase in energy too.

## 5. Conclusion

A ray tracing tool to analyze a solar concentrating system has been presented. The model simulates the sun emitting rays and traces them up to the final destination on the receiver or when they are lost in the surrounding. The performance of the parabolic dish using a continuous reflecting surface and flat mirror tiles has been explored and found out that a continuous surface has better performance. Errors in tracking mechanisms have been illustrated by the ray tracer tool and the use of a secondary reflector to improve the fraction of the reflected rays reaching the receiver has also been demonstrated. The ray tracer tool could be used in designing solar concentrating systems.

## Acknowledgement

We are grateful to NUFU for supporting this work.

## 6. Reference

1. Chikukwa A., 2007. Modelling of a Solar Stove : Small concentrating system with a heat storage. PhD thesis, Norwegian University of Science & Technology.
2. Chi-Feng Chena, Chih-Hao Lina, Huang-TzungJan, 2010. A solar concentrator with two reflection mirrors designed by using array tracing method. *Optik*, 121:1042–1051.
3. Duffie J.A., Beckman W.A., 2006. *Solar Engineering of Thermal Processes*. John Wiley and Sons, Inc. 2nd edition.
4. Ralf Leutz, Hans Philipp Annen, 2007. Reverse ray-tracing model for the performance evaluation of stationary solar concentrators. *Solar Energy*, 81:761–767.
5. Seron F.J., Gutierrez D., Gutierrez G., Cerezo E., 2005. Implementation of a method of curved raytracing for inhomogeneous atmospheres. *Computers & Graphics*, 29:95–108.
6. Spencer G.H., Murty M.V.R.K., 1962, General ray-tracing procedure. *Journal of the Optical Society of America*, 52:630–678.
7. Stephen W., Lars Oliver-Grobe, David Geisler Moroder, Raphael Compagnon, Jerome Kampf, Friedrich Linhart, Jean-Louis Scartezzini, 2010. Ray tracing study for non-imaging daylight collectors. *Solar Energy*, 84:986–996.
8. Te-Tan Liao, 2009. A skew ray tracing approach for the error analysis of optical elements with paraboloidal boundary surfaces. *Optik*, 120:873–885.
9. Yevgen Grynko, Yuriy Shkuratov, 2007. Ray tracing simulation of light scattering by spherical clusters consisting of particles with different shapes. *Journal of Quantitative Spectroscopy & Radiative Transfer*, 106:56–62.
10. Zeng Xiangyang, Chen Kean, Sun Jincai, 2003. On the accuracy of the ray-tracing algorithms based on various sound receiver models. *Applied Acoustics*, 64:433–441.